MDPI sciforum

MOL2NET, International Conference Series on Multidisciplinary Sciences

Virtual screening based on covalent docking and MM-PBSA calculations predict the drugs neratinib, sacubitril, alprostadil, trandolapril, and florbetapir as promising cruzain inhibitors useful against Chagas disease.

Lucas Gabriel dos Santos Costa[a], *Thiago Mendonça de Aquino*[b], *and Igor José dos Santos Nascimento*[a*]

[a]*Estácio of Alagoas College, Pharmacy Department, Maceió-AL, Brazil*

[b] *Laboratory of Computational Chemistry and Biomolecule Modeling, Federal University of Alagoas, Maceio-AL, Brazil*

* *Corresponding Author: igorjsn@hotmail.com*

Graphical Abstract:

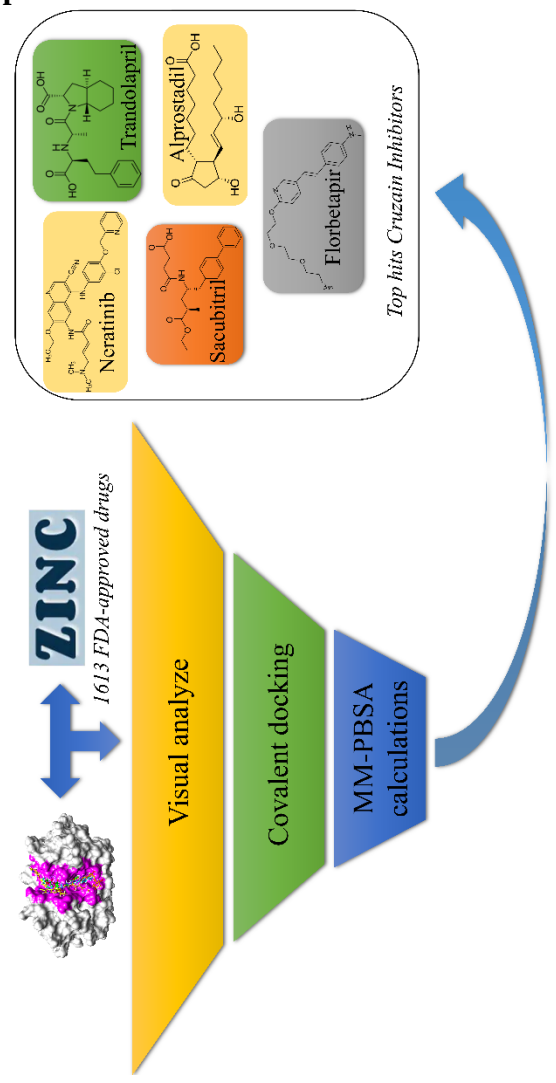

Abstract. This work aimed to perform a virtual screening using a covalent docking and MM-PBSA protocol in an FDA-approved drugs library dataset to search for new compounds useful against this cruzain. Initially, 1615 FDA-approved compounds were visually inspected for the presence of chemical groups reactive against cruzain reactive cysteine (Cys^{25}), followed by the choice of the most suitable 3D structure for the virtual protocols. Thus, 241 compounds were selected and the covalent docking assays and the drugs with a fit score covalent greater than 100, were selected to the MM-PBSA calculations. Finally, the drugs neratinib, sacubitril, alprostadil, trandolapril, and florbetapir showed a covalent fit score between 102.14 and 116.59; $\Delta G_{binding}$ values between -72.851 and -148,811 Kcal/mol calculated by MM-PBSA; and interactions with the key residues of the cruzain (Cys^{25}, His^{159}, Gly^{23}, and Gly^{65}), showing best values than other cruzain inhibitors experimentally assayed. Our findings suggest that these drugs may be possible cruzain inhibitors, and biological assays should be performed to confirm their potential.

1. Introduction

Neglected tropical diseases (NTD) are groups of parasitic and bacterial disorders that affect over 149 countries of subtropical conditions [1]. These agents are more prevalent in the population living in poverty without basic sanitation, indicative of social marginalization, causing harm to countries' economies [1,2]. Public health policies related to control prevention are the main measures taken to avoid such diseases [1]. Among these, Chagas disease has been causing concern in health agencies worldwide due to the growing number of cases in recent years, endemic in more than 21 countries, with estimates of approximately 6 to 7 million infected, and 75 million in risk situation [1]. Despite presenting alarming data, there are only two drugs approved for the treatment (nifurtimox and benznidazole), being a challenge for medicinal chemists worldwide to discover a new innovative treatment [3].

Among the most explored targets in drug design in the search for new drugs against Chagas disease is cruzain [3]. This enzyme is key in several biochemical processes of the parasite, such as invasion, differentiation, proliferation, and degradation of host cell proteins, contributing to the infectious process [4]. Furthermore, cruzain is found in all stages of the parasite's life cycle (epimastigotes, trypomastigotes, metacyclic trypomastigotes, and amastigotes), becoming an excellent drug target in studies against Chagas disease [5,6].

In recent years, the strategy of discovering new drugs through drug repurposing has gained great prominence [7–9]. Through this method, it is possible to find new clinical indications for drugs approved for clinical use, or even drugs that already form clinical candidates, which have a clinically proven safety and efficacy profile. The advantage of repurposing a drug is that it avoids future problems related to toxicity and inadequate pharmacokinetics. This approach linked to bioinformatics, through *in silico* methods accelerates the discovery process and increases the probability of success in a new drug discovery campaign. [10,11].

Finally, based on the above information, a virtual drug repositioning screening campaign was carried out here using a library of 1615 FDA-approved drugs employing a covalent docking protocol and MM-PBSA calculations. From this source, it was found that the drugs neratinib, sacubitril, alprostadil, trandolapril, and florbetapir showed a covalent fit score between 102.14 and 116.59; $\Delta G_{binding}$ values between -72,851 and -148,811 Kcal/mol calculated by MM-PBSA; and interactions with the key residues of the cruzain (Cys^{25}, His^{159}, Gly^{23}, and Gly^{65}), showing better values than other cruzain inhibitors experimentally assayed. Our findings suggest that these drugs may be possible cruzain inhibitors, and biological assays should be performed to confirm their potential.

2. Materials and Methods

2.1 Target selection and preparation

To select the best 3D structures, 18 cruzain co-crystallized with a covalent inhibitor were obtained using the database Research Collaboratory for Structural Bioinformatics Protein Data Bank database (RCSB PDB, https://www.rcsb.org/) [12]. Hydrogens were added for each of these structures, and co-crystallized ligands were removed and, subsequently, submitted to our re-docking procedure in

a covalent approach, using *GOLD*® v. 5.8.1 software [13]. The re-docking was performed by using all four algorithms, being Chemical Piecewise Linear Potential (ChemPLP), GoldScore, ChemScore, and Astex Statistical Potential (ASP). The best-fit pose was chosen for each ligand, and its value of Root-Mean-Square Deviation (RMSD) was calculated by using the *PyMol*® software [14]. Finally, a heat-map was generated through *Microsoft Excel*®. Thus, was chosen the most accurate structure for virtual screening simulations after our Re-docking procedures (with the lowest RMSD value). Finally, the structure 1EWO (PDB id) [15] was chosen and used in the covalent docking protocol.

2.2 Selection and preparation of ligand dataset

From the ZINC database (https://zinc.docking.org/), 1,615 FDA-approved drugs were visually inspected to the presence of chemically reactive groups against the Cys25 from cruzain. In this way, 241 were selected and, submitted to the conformational analysis using the *MarvinSketch*® software [16]. Thus, ten conformations were generated for each ligand, begin choosing the conformation having the lowest energy value. The molecules were then minimized using the *ArgusLab*® software [17] by applying the semi-empirical AM1 (Austin Model 1).

2.3 Covalent docking

Covalent docking studies were performed using the *GOLD*® software by employing the ChemPLP algorithm (chosen after the validation procedure). Initially, was performed a conventional molecular docking, in a six Å region around the co-crystallized ligand and selected the maximum efficiency of the genetic algorithm (GA). Finally, ten binding poses were generated for each ligand, in which the most excellent fit score was chosen. With the complex obtained, the covalent bond between the electrophile group of the ligand and Cys^{25} was created using *Discovery Studio*® software [26]. Finally, the covalent docking using *GOLD*® software was performed, selecting the electrophilic group of the ligand and the sulfur atom of Cys^{25} in the same protocol described for conventional docking, generating ten complexes, in which, the most significant fit score was selected for the MM-PBSA calculations.

2.4 Molecular dynamics simulations

The trajectory files for the MM-PBSA calculations were obtained through Molecular dynamic simulations performed by using the *GROMACS*® software. All complexes were obtained through molecular docking studies. Thus, water molecules were removed, while charges and hydrogens were added, using the *DockPrep* tool from the *Chimera*® software. Then, the CHARMM36 force field was employed, followed by the TIP3P solvation method. Ligand topologies were generated by web software *SwissParam* (http://www.swissparam.ch/) [18]. Thus, a 1.0 nm triclinic box was created, adding water and ions at the physiological concentration (0.15M). The system was initially equilibrated in 10,000 steps by the conjugate gradient method, followed by the system's total minimization in 20,000 steps. Then, NVT (constant Number of particles, Volume, and Temperature) and NPT (constant Number of particles, Pressure, and Temperature) balances were performed at a temperature of 300 K, during ten ns. The 10 ns simulation runs were performed with the free protein and complexed with the top-hit ligands with the system assembled. Finally, the tpr and xtc files were

used in MM-PBSA calculations. These files were used for choosing the most stable conformation, using the tool *MD movie*, and *cluster analysis* in the *Chimera*® software.

2.5 MM-PBSA calculations

Molecular Mechanics/Poisson-Boltzmann Surface Area (MM-PBSA) method calculates the energy of interactions between ligand and a macromolecule. These calculations are generally applied in high-throughput virtual screenings to reduce false positives [19]. Thus, this method calculates the Gibbs free-biding energy ($\Delta G_{binding}$) based on van der Waals and electrostatic (unbound) interactions between the ligand and its receptor during a molecular dynamics simulation [20]. Thus, the $\Delta G_{binding}$ is calculated by the difference between the free energy of complex protein-ligand (G_{cpx}) and unbound protein and ligand (G_{rec}). Finally, the $\Delta G_{binding}$ was considerate such as summation of the changes in the solvation entropy ($-T\Delta S_{sol}$), binding energy (ΔE_{bind}) and conformational entropy ($-T\Delta S_{conf}$), as shown in equation 1 [21]. MM-PBSA calculations were performed using the *g_mmpbsa* tool [19] through the trajectory files obtained after the molecular dynamics simulation at 100 ns, using the *GROMACS*® software. Then, $\Delta G_{binding}$ values were determined as the average of free-interaction and solvation energies [20].

$$\Delta G_{binding} = E_{binding} - T\Delta S_{sol} - T\Delta S_{conf} \qquad (Equation\ 1)$$

2.5 Interaction analyses of most stable conformation.

After the protocol of molecular dynamics, the most stable conformation of each complex was analyzed for their interactions with the key residues (Cys^{25}, His^{159}, Gly^{23}, and Gly^{65}) using the *Discovery Studio*® software [22]. The 3D figure interactions were generated using the *Chimera*® software [23].

3. Results and Discussion

3.1 Screening protocol validation

For validation of screening protocol, was performed a re-docking in a covalent docking protocol of 18 crystal structures of the cruzain available in the PDB database using the four algorithms (ChemPLP, GoldScore, ChemScore, and ASP) of the *GOLD*® software. This procedure is according to other previously published by our research group [24–26]. Thus, the RMSD of the ligands was calculated and the PDB 1EWO in the algorithm ChemPLP was chosen, showing the best RMDS value (0.275) between the ligand docked and co-crystalized. Next, this crystal structure was used in a covalent docking protocol of the 18 ligands co-crystallized in available in the PDB database. The ligands showed a fit score between 49.85 - 94.18 (Table **1**), and a covalent fit score varying between 49.91 – 141.52 (Table 1). In addition, it was observed that the compounds with conventional fit score and covalent fit score better than 55 and 90, respectively, showed interactions with the main residues related to the cruzain inhibition (Cys^{25}, His^{159}, Glu^{23}, Gly^{65}, and Glu^{205})[3,5,6,26,27] (Table **1**). Other works used a similar protocol to search new hits to drug design [10,28,29]. In this way, these values were used as a start point to filter the drugs in the virtual screening covalent docking-based (next section).

Table 1. Dataset collection of crystalized covalent inhibitors for protocol validation.

PDB id	Ligand	Fit score	Main Interactions					Covalent score
			Gly^{23}	Cys^{25}	Gly^{65}	Glu^{205}	His^{159}	
2AIM	ZRA	71.98	C-H-bond	H-bond	VDW	VDW	H-bond	95.07
1AIM	ZYA	74.86	C-H-bond	VDW	C-H-bond	VDW	H-bond	112.33
1EWM	RL2	60.85	VDW	VDW	C-H-bond	VDW	VDW	97.73
1EWO	VSC	90.59	C-H-bond	π-alkyl	C-H-bond	VDW	amide-π	129.03
1EWL	R99	61.72	C-H-bond	VDW	C-H-bond	VDW	amide-π	99.78
4PI3	2V5	75.08	VDW	VDW	H-bond	---	amide-π	122.45
1EWP	0I5	61.79	VDW	H-bond	C-H-bond	---	VDW	62.47
3I06	QL2	49.85	---	H-bond	C-H-bond	C-H-bond	VDW	63.44
3IUT	KB2	89.68	C-H-bond	π-sulfur	amide-π	---	π-alkyl	104.40
4QH6	33L	56.54	VDW	VDW	C-H-bond	VDW	amide-π	95.26
3LXS	4MC	82.62	C-H-bond	π-alkyl	amide-π	VDW	π-alkyl	134.22
1F2B	VS3	94.18	C-H-bond	C-H-bond	C-H-bond	VDW	C-H-bond	49.91
1F2A	VS2	86.61	C-H-bond	H-bond	C-H-bond	VDW	VDW	140.93
1F29	VS1	78.16	VDW	H-bond	C-H-bond	VDW	H-bond	141.52
1F2C	VS4	91.93	C-H-bond	H-bond	C-H-bond	VDW	H-bond	88.57
7JUJ	GN9	65.09	H-bond	π-alkyl	C-H-bond	---	π-alkyl	100.04
6UX6	TM8	81.95	VDW	π-alkyl	VDW	---	H-bond	115.92
3HD3	25B	73.25	C-H-bond	VDW	C-H-bond	---	H-bond	128.23

3.2 Virtual screening covalent docking-based

With PDB crystal structure, *GOLD*® algorithm selected and the start point values for screening the drugs, the next stage was built the ligand dataset. For this, 1615 FDA-approved drugs from the ZINC database were visually analyzed for choosing the drugs with chemical groups that can interact covalently with the sulfur atom of Cys^{25} from cruzain [3]. This analysis resulted in the selection of 241 drugs that contained ester, carbon α-halogenated, nitrile, amide, and alkenes, and alkyne. The covalent docking was performed in this dataset, resulting in the selection of 10 compounds with conventional fit score and covalent fit score better than 55 and 90, respectively (Table **2**) and interactions with the key residues (Table **2**), similar to the know inhibitors showed in Table **1**.

Interestingly, our screening protocol was able to identify drugs of the most diverse therapeutical indication and with previously known anti-*Trypanosoma* activity. The drugs ZINC1853205 (trandolapril) and ZINC3792417 (sacubitril) are inhibitors of the angiotensin-converting enzyme (ACE), and the ZINC29319828 (eprosartan) is an angiotensin receptor blocker, in which several pieces of evidence indicate that this therapeutics class shows benefices against chronic infection of *Trypanosoma cruzi* [30–34]. Furthermore, ZINC1536109 (pralatrexate) and ZINC3916214 (neratinib) are anticancer drugs, in which evidence point that the first is a solute carrier proteins (SLCs) inhibitor, similar to pentamidine, a drug used against African trypanosomiasis, and can be useful against the Chagas diseases [35,36]. On other hand, the ZINC3916214 (neratinib) is used against HER2* breast cancer with an electrophilic group that some authors associate as cysteine proteases inhibitor [36]. In addition, the drug ZINC4098633 (polydatin) is a resveratrol glucoside, and the resveratrol is a known compound with anti-*Trypanosoma cruzi* activity [37,38]. Other drugs with known activity are ZINC1530575 (capsaicin), previously identified as a Trypanosoma cruzi arginine kinase (TcAK) inhibitor, and can be promising results in biological assays against this disease [39]. Finally, the drugs ZINC3813078 (epoprostenol), ZINC3813088 (alprostadil), ZINC43207237 (florbetapir) are prostacyclin analog, a prostaglandin analog, and positron emission tomography (PET), respectively, that can be explored their potential against cruzain and Chagas diseases [40–42].

Table 2. The fit score of conventional and covalent docking, and main interactions of top 10 compounds from virtual screening protocol.

ZINC code	Drug	Fit score		Main Interactions				
		Conventional	Covalent	Gly^{23}	Cys^{25}	Gly^{65}	Glu^{205}	His^{159}
ZINC3813078	Epoprostenol	62.86	102.12	VDW	VDW	C-H-bond	VDW	VDW
ZINC1530575	Capsaicin	62.29	114.32	VDW	C-H-bond	C-H-bond	VDW	C-H-bond
ZINC1536109	Pralatrexate	65.81	90.94	C-H-bond	H-bond	C-H-bond	VDW	H-bond
ZINC1853205	Trandolapril	58.63	116.14	C-H-bond	H-bond	C-H-bond	VDW	VDW
ZINC3792417	Sacubitril	64.90	107.87	VDW	π-alkyl	VDW	VDW	H-bond
ZINC3813088	Alprostadil	66.77	105.68	VDW	VDW	C-H-bond	VDW	H-bond
ZINC3916214	Neratinib	73.46	102.14	H-bond	H-bond	VDW	C-H-bond	C-H-bond
ZINC4098633	Polydatin	57.96	103.68	C-H-bond	H-bond	VDW	VDW	VDW
ZINC29319828	Eprosartan	65.65	116.21	C-H-bond	π-Sulfur	C-H-bond	VDW	VDW
ZINC43207237	Florbetapir	67.24	116.59	C-H-bond	π-alkyl	VDW	H-bond	H-bond

3.3 MM-PBSA calculations

The MM-PBSA calculations were performed to re-score the best drugs identified here, and the results are shown in Table **3**. The drug neratinib shows de best free binding energy, with a high $\Delta G_{binding}$ of -148.811 ± 15.601 kJ/mol, followed by the drugs trandolapril, florbetapir, sacubitril, and alprostadil ($\Delta G_{binding}$ value of -94.222 ± 15.615, -93.683 ± 15.577, -77.117 ± 15.489, and -72.851 ± 32.564 kJ/mol, respectively). The high free binding energy values indicate that the drugs can be useful against cruzain. These results are according to other works, such as Silva *et al.*, [26], in which their most potent cruzain inhibitor shows an $\Delta G_{binding}$ value of -50.71 kJ/mol. In addition, the other drugs identified pralatrexate and polydatin showed great free binding energy values ($\Delta G_{binding}$ value of -67.445 ± 26.952, and -54.591 ± 14.666 kJ/mol, respectively), and can be evaluated to determine their potential. The drugs epoprostenol, capsaicin, and eprosartan ($\Delta G_{binding}$ value of -34.764 ± 43.137, -19.080 ± 58.756, and 446.749 ± 25.311 kJ/mol, respectively) showed the low values. Our findings indicate that the drugs can be investigated in biological assay and offer promising results.

In addition to the free binding energy, the drugs were analyzed concerning the main interactions involved in the formation of the drug-cruzain complex. Interesting, the drugs with the most affinity to the cruzain (neratinib, trandolapril, and florbetapir) showed the best SASA energy value (-21.582 ± 1.225, -17.836 ± 1.200, -17.967 ± 2.242 kJ/mol, respectively), indicating bigger permanence in a hydrophobic environment, away from the external environment exposed to solvent, which can be related to the most excellent affinity to the target [43]. On the other hand, the drugs epoprostenol, capsaicin showed high SASA energy values (-6.101 ± 6.184, and -4.324 ± 5.591 kJ/mol), justifying the low affinity. Also, all drugs showed the values of Van der Waals energy better than electrostatic energy (see Table **3**), which indicates that van der Walls interactions are the most important to the formation of the drug-enzyme complex [44]. Finally, the polar solvation energy with positive values (see Table **3**) and high electrostatic energy suggest that the polar contribution is unfavorable to the binding processes of these drugs with the cruzain [45]. Thus, these finding indicates new insight about chemical compounds that can be affinity to this target.

The top 5 hit compounds (neratinib, sacubitril, alprostadil, trandolapril, and florbetapir) were calculated the contribution energy *per*-residue by MM-PBSA to determine the mains related to the interaction process, shown in Figure **1**. In fact, all top show the Cys^{25} as the best energy (between -1.14 and -3.29 kJ/mol), suggesting the strong interactions with this residue. Besides, other residues such as Leu^{67} (between -2.12 and -7.34 kJ/mol), Asp^{135} (between -2.89 and -3.79 kJ/mol) showed their importance in forming the complex. Authors such as Wiggers *et al.* [46] highlight the importance of the interaction with these residues to the cruzain inhibition. Finally, the drug of the most affinity energy (neratinib) showed great interaction with Gln^{23} (-3.58), Cys^{25} (-3.24), His^{159} (-3.80), Glu^{205} (-5.13), and other residues, which contribute to the most excellent affinity.

Table 3. MM-PBSA results of the top 10 drugs selected in the covalent virtual screening.

ZINC code	Drug	Binding Energy (kJ/mol)	SASA Energy (kJ/mol)	Polar Solvation Energy (kJ/mol)	Electrostatic Energy (kJ/mol)	Van der Waals Energy (kJ/mol)
ZINC3813078	Epoprostenol	-34.764 ± 43.137	-6.101 ± 6.184	26.775 ± 52.942	-14.152 ± 24.238	-41.287 ± 42.624
ZINC1530575	Capsaicin	-19.080 ± 58.756	-4.324 ± 5.591	21.199 ± 51.087	-4.732 ± 9.922	-31.224 ± 42.724
ZINC1536109	Pralatrexate	-67.445 ± 26.952	-13.209 ± 3.501	100.194 ± 40.274	-49.389 ± 25.459	-105.040 ± 43.196
ZINC1853205	Trandolapril	-94.222 ± 15.615	-17.836 ± 1.200	122.788 ± 20.256	-44.292 ± 10.988	-154.882 ± 11.637
ZINC3792417	Sacubitril	-77.117 ± 15.489	-14.158 ± 1.869	76.046 ± 24.701	-9.639 ± 13.584	-129.367 ± 15.793
ZINC3813088	Alprostadil	-72.851 ± 32.564	-13.655 ± 1.392	80.931 ± 36.936	-46.775 ± 19.642	-93.353 ± 16.024
ZINC3916214	Neratinib	-148.811 ± 15.601	-21.582 ± 1.225	118.969 ± 21.009	-31.990 ± 12.750	-214.207 ± 15.326
ZINC4098633	Polydatin	-54.591 ± 14.666	-16.060 ± 1.685	137.905 ± 26.958	-51.707 ± 24.565	-124.728 ± 16.439
ZINC29319828	Eprosartan	446.749 ± 25.311	-10.661 ± 1.551	28.478 ± 32.186	479.619 ± 34.944	-50.687 ± 14.493
ZINC43207237	Florbetapir	-93.683 ± 15.577	-17.967 ± 2.242	104.368 ± 33.073	-20.398 ± 15.505	-159.686 ± 22.722

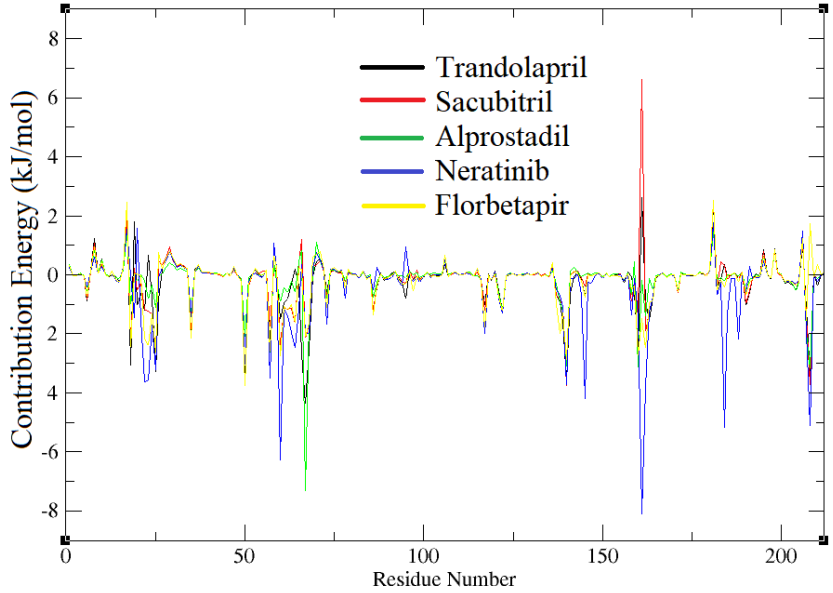

Figure 1. Contribution energy plot *per*-residue calculate through MM-PBSA for trandolapril (black line); sacubitril (red line); alprostadil (green line), neratinib (blue line); and florbetapir (yellow line).

3.4 Interaction analysis of top 5 hits at the active site

Using the trajectory of the molecular dynamics simulations, the cluster analyses were performed for choosing the most stable conformation, following the interaction analysis at the active site of cruzain shown in Figure **2**. The drug neratinib showed strong interactions with Cys^{25} (H-bond) and His^{159} (C-H-bond) related to the catalytic activity of this target, justifying the most excellent affinity. In addition, the compounds interacted with other residues, such Leu^{67} (VDW), Asp^{158} (VDW), and Ala^{133} (VDW) similar to known inhibitors [47,48]. All drugs showed interactions with Ala133, Asp158, Leu67, similar to the findings of Cardoso *et al.* [48], in which their compounds exhibited IC_{50} between 0.01 and 9.3 μM against cruzain. These results suggested that the compounds can be promising in biological assays.

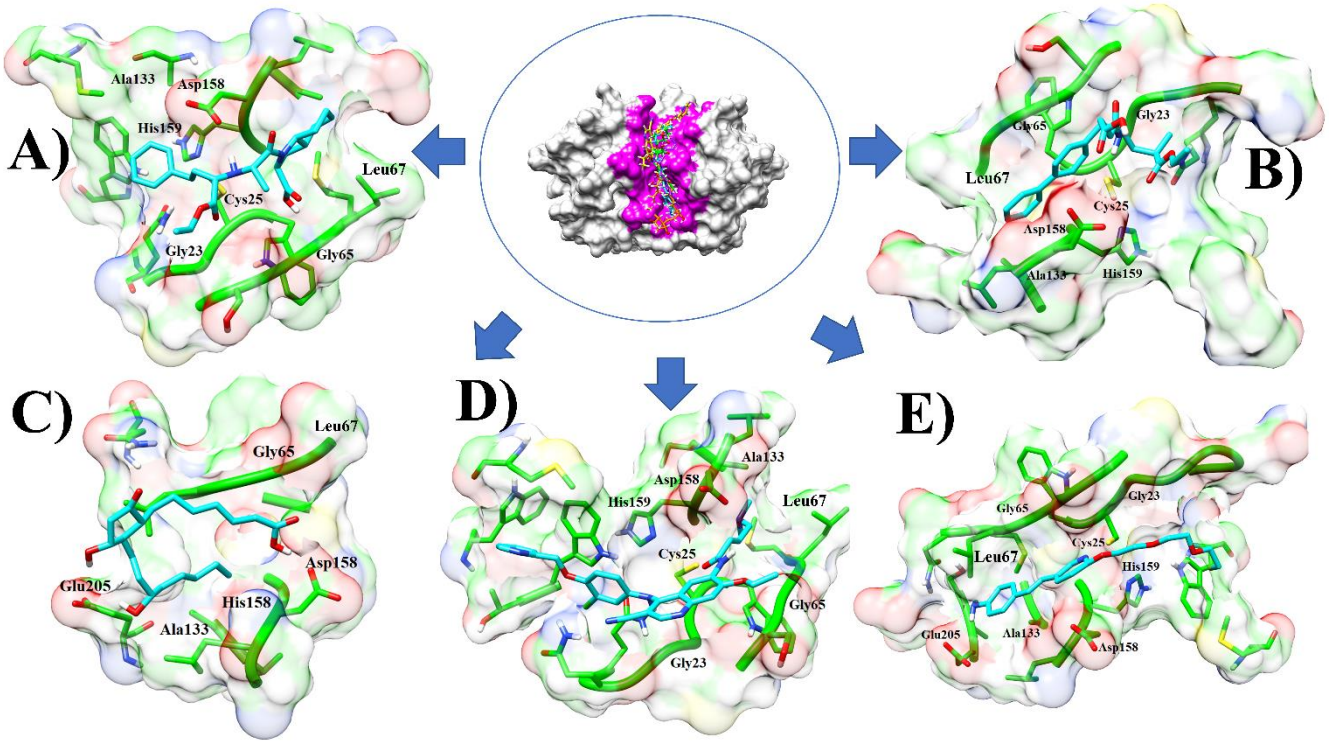

Figure 2. Interactions of the most stable conformation of top hits at the active site of cruzain after molecular dynamics: A) trandolapril; B) sacubitril; C) alprostadil; D) neratinib; E) florbetapir.

4. Conclusions

The discovery of a new drug against the Chagas disease is one of the main efforts of medicinal chemistry. Despite the existence of treatments against this disease, the drugs showed high toxicity and in the chronic stage of infections are ineffective. Here, a virtual drug repurposing screening was able to identify new drugs that can be overcome several challenges in new treatments for Chagas disease. In fact, the drugs neratinib, sacubitril, alprostadil, trandolapril, and florbetapir showed the best results employing a protocol based on covalent docking and MM-PBSA calculations, similar to the experimental data of known inhibitors. These findings suggest new drugs that can be evaluated in vitro and in vivo assay, to prove their potential anti-Chagas disease.

Acknowledgments

The authors thank the Coordenação de Aperfeiçoamento de Pessoal de Nível Superior – Brazil (CAPES) and the National Council for Scientific and Technological Development (CNPq) – Brazil for their support to the Brazilian Post-Graduate Programs. In addition, the authors would like thanks to the "Centro Nacional de Processamento de Alto Desempenho em São Paulo (CENAPAD-SP) for using their resources.

Declaration of interest

The authors have no relevant affiliations or financial involvement with any organization or entity with a financial interest in or financial conflict with the subject matter or materials discussed in the manuscript. This includes employment, consultancies, honoraria, stock ownership or options, expert testimony, grants or patents received or pending, or royalties.

References

[1] WHO | World Health Organization. *WHO*, **2020**.
[2] Chami, G.F.; Bundy, D.A.P. More Medicines Alone Cannot Ensure the Treatment of Neglected Tropical Diseases. *Lancet Infect. Dis.*, **2019**, *19*, e330–e336.
[3] Santos Nascimento, I.J. dos; de Aquino, T.M.; da Silva-Júnior, E.F. Cruzain and Rhodesain Inhibitors: Last Decade of Advances in Seeking for New Compounds Against American and African Trypanosomiases. *Curr. Top. Med. Chem.*, **2021**, *21*.
[4] Magalhaes Moreira, D.R.; De Oliveira, A.D.T.; Teixeira De Moraes Gomes, P.A.; De Simone, C.A.; Villela, F.S.; Ferreira, R.S.; Da Silva, A.C.; Dos Santos, T.A.R.; Brelaz De Castro, M.C.A.; Pereira, V.R.A.; Leite, A.C.L. Conformational Restriction of Aryl Thiosemicarbazones Produces Potent and Selective Anti-Trypanosoma Cruzi Compounds Which Induce Apoptotic Parasite Death. *Eur. J. Med. Chem.*, **2014**, *75*, 467–478.
[5] Ferreira, L.G.; Andricopulo, A.D. Targeting Cysteine Proteases in Trypanosomatid Disease Drug Discovery. *Pharmacol. Ther.*, **2017**, *180*, 49–61.
[6] Scarim, C.B.; Jornada, D.H.; Chelucci, R.C.; de Almeida, L.; dos Santos, J.L.; Chung, M.C. Current Advances in Drug Discovery for Chagas Disease. *Eur. J. Med. Chem.*, **2018**, *155*, 824–838.
[7] dos Santos Nascimento, I.J.; de Aquino, T.M.; da Silva-Júnior, E.F. Drug Repurposing: A Strategy for Discovering Inhibitors against Emerging Viral Infections. *Curr. Med. Chem.*, **2021**, *28*, 2887–2942.
[8] José dos Santos Nascimento, I.; Mendonça de Aquino, T.; Fernando da Silva Santos-Júnior, P.; Xavier de Araújo-Júnior, J.; Ferreira da Silva-Júnior, E. Molecular Modeling Applied to Design of Cysteine Protease Inhibitors – A Powerful Tool for the Identification of Hit Compounds Against Neglected Tropical Diseases. In: *Frontiers in Computational Chemistry*; **2020**; Vol. 5, pp. 63–110.
[9] dos Santos Nascimento, I.J.; da Silva-Júnior, E.F.; de Aquino, T.M. Molecular Modeling Targeting Transmembrane Serine Protease 2 (TMPRSS2) as an Alternative Drug Target Against Coronaviruses. *Curr. Drug Targets*, **2021**, *22*.
[10] Bellera, C.L.; Balcazar, D.E.; Vanrell, M.C.; Casassa, A.F.; Palestro, P.H.; Gavernet, L.; Labriola, C.A.; Gálvez, J.; Bruno-Blanch, L.E.; Romano, P.S.; Carrillo, C.; Talevi, A.

Computer-Guided Drug Repurposing: Identification of Trypanocidal Activity of Clofazimine, Benidipine and Saquinavir. *Eur. J. Med. Chem.*, **2015**, *93*, 338–348.

[11] Bellera, C.L.; Balcazar, D.E.; Alberca, L.; Labriola, C.A.; Talevi, A.; Carrillo, C. Application of Computer-Aided Drug Repurposing in the Search of New Cruzipain Inhibitors: Discovery of Amiodarone and Bromocriptine Inhibitory Effects. *J. Chem. Inf. Model.*, **2013**, *53*, 2402–2408.

[12] BERNSTEIN, F.C.; KOETZLE, T.F.; WILLIAMS, G.J.B.; MEYER, E.F.; BRICE, M.D.; RODGERS, J.R.; KENNARD, O.; SHIMANOUCHI, T.; TASUMI, M. The Protein Data Bank. A Computer-Based Archival File for Macromolecular Structures. *Eur. J. Biochem.*, **1977**, *80*, 319–324.

[13] Verdonk, M.L.; Cole, J.C.; Hartshorn, M.J.; Murray, C.W.; Taylor, R.D. Improved Protein-Ligand Docking Using GOLD. *Proteins Struct. Funct. Bioinforma.*, **2003**, *52*, 609–623.

[14] Lill, M.A.; Danielson, M.L. Computer-Aided Drug Design Platform Using PyMOL. *J. Comput. Aided. Mol. Des.*, **2011**, *25*, 13–19.

[15] Brinen, L.S.; Gillmor, S.A.; Fletterick, R.J. THE CYSTEINE PROTEASE CRUZAIN BOUND TO WRR-204. *Protein Data Bank*, **2000**.

[16] Csizmadia, P. *MarvinSketch and MarvinView: Molecule Applets for the World Wide Web* In: Proceedings of the Proceedings of The 3rd International Electronic Conference on Synthetic Organic Chemistry; MDPI: Basel, Switzerland, **1999**; p. 1775.

[17] Oda, A.; Okayasu, M.; Kamiyama, Y.; Yoshida, T.; Takahashi, O.; Matsuzaki, H. Evaluation of Docking Accuracy and Investigations of Roles of Parameters and Each Term in Scoring Functions for Protein–Ligand Docking Using ArgusLab Software. *Bull. Chem. Soc. Jpn.*, **2007**, *80*, 1920–1925.

[18] Zoete, V.; Cuendet, M.A.; Grosdidier, A.; Michielin, O. SwissParam: A Fast Force Field Generation Tool for Small Organic Molecules. *J. Comput. Chem.*, **2011**, *32*, 2359–2368.

[19] Kumari, R.; Kumar, R.; Lynn, A. G_mmpbsa —A GROMACS Tool for High-Throughput MM-PBSA Calculations. *J. Chem. Inf. Model.*, **2014**, *54*, 1951–1962.

[20] Sarma, H.; Mattaparthi, V.S.K. Structure-Based Virtual Screening of High-Affinity ATP-Competitive Inhibitors Against Human Lemur Tyrosine Kinase-3 (LMTK3) Domain: A Novel Therapeutic Target for Breast Cancer. *Interdiscip. Sci. Comput. Life Sci.*, **2019**, *11*, 527–541.

[21] Wang, F.; Wu, F.-X.; Li, C.-Z.; Jia, C.-Y.; Su, S.-W.; Hao, G.-F.; Yang, G.-F. ACID: A Free Tool for Drug Repurposing Using Consensus Inverse Docking Strategy. *J. Cheminform.*, **2019**, *11*, 73.

[22] Wang, Q.; He, J.; Wu, D.; Wang, J.; Yan, J.; Li, H. Interaction of α-Cyperone with Human Serum Albumin: Determination of the Binding Site by Using Discovery Studio and via Spectroscopic Methods. *J. Lumin.*, **2015**, *164*, 81–85.

[23] Goddard, T.D.; Huang, C.C.; Ferrin, T.E. Software Extensions to UCSF Chimera for Interactive Visualization of Large Molecular Assemblies. *Structure*, **2005**, *13*, 473–482.

[24] Santana, C.C.; Silva-Júnior, E.F.; Santos, J.C.N.; Rodrigues, É.E. da S.; da Silva, I.M.; Araújo-Júnior, J.X.; do Nascimento, T.G.; Oliveira Barbosa, L.A.; Dornelas, C.B.; Figueiredo, I.M.; Santos, J.C.C.; Grillo, L.A.M. Evaluation of Guanylhydrazone Derivatives as Inhibitors of Candida Rugosa Digestive Lipase: Biological, Biophysical, Theoretical Studies and Biotechnological Application. *Bioorg. Chem.*, **2019**, *87*, 169–180.

[25] dos Santos Nascimento, I.J.; da Silva-Júnior, E.F. TNF-α Inhibitors from Natural Compounds: An Overview, CADD Approaches, and Their Exploration for Anti-Inflammatory Agents. *Comb. Chem. High Throughput Screen.*, **2021**, *24*.

[26] Silva, L.R.; Guimarães, A.S.; do Nascimento, J.; do Santos Nascimento, I.J.; da Silva, E.B.; McKerrow, J.H.; Cardoso, S.H.; da Silva-Júnior, E.F. Computer-Aided Design of 1,4-Naphthoquinone-Based Inhibitors Targeting Cruzain and Rhodesain Cysteine Proteases. *Bioorg. Med. Chem.*, **2021**, *41*, 116213.

[27] da Silva-Junior, E.F.; Barcellos Franca, P.H.; Ribeiro, F.F.; Bezerra Mendonca-Junior, F.J.; Scotti, L.; Scotti, M.T.; de Aquino, T.M.; de Araujo-Junior, J.X. Molecular Docking Studies Applied to a Dataset of Cruzain Inhibitors. *Curr. Comput. Aided. Drug Des.*, **2017**, *14*, 68–78.

[28] Passos, G.F.S.; Gomes, M.G.M.; Aquino, T.M. de; Araújo-Júnior, J.X. de; Souza, S.J.M. de;

Cavalcante, J.P.M.; Santos, E.C. dos; Bassi, Ê.J.; Silva-Júnior, E.F. da. Computer-Aided Design, Synthesis, and Antiviral Evaluation of Novel Acrylamides as Potential Inhibitors of E3-E2-E1 Glycoproteins Complex from Chikungunya Virus. *Pharmaceuticals*, **2020**, *13*, 141.

[29] Herrera-Mayorga, V.; Lara-Ramírez, E.; Chacón-Vargas, K.; Aguirre-Alvarado, C.; Rodríguez-Páez, L.; Alcántara-Farfán, V.; Cordero-Martínez, J.; Nogueda-Torres, B.; Reyes-Espinosa, F.; Bocanegra-García, V.; Rivera, G. Structure-Based Virtual Screening and In Vitro Evaluation of New Trypanosoma Cruzi Cruzain Inhibitors. *Int. J. Mol. Sci.*, **2019**, *20*, 1742.

[30] Shrestha, D.; Penitente, A.R.; Horta, A.L.; Leite, A.L.J.; Neves, C.A.; Natali, A.J.; de Paula Costa, G.; Talvani, A. Enalapril in Combination with Benznidazole Reduces Cardiac Inflammation and Creatine Kinases in Mice Chronically Infected with Trypanosoma Cruzi. *Am. J. Trop. Med. Hyg.*, **2015**, *93*, 976–982.

[31] Cutz Ijchajchal, M.A.; Eva Lopez, M.L.; Aceituno Melgar, J.E.; Hernández Marroquín, J.J.; Penagos Cordón, J.C. Chagas Cardiomyopathy: Evidence in Medical and Nutritional Management. *Curr. Trop. Med. Reports*, **2018**, *5*, 193–203.

[32] Souza-Silva, T.G.; Diniz, L.F.; Lia Mazzeti, A.; Mendonça, A.A.S.; Gonçalves, R. V.; Novaes, R.D. Could Angiotensin-Modulating Drugs Be Relevant for the Treatment of Trypanosoma Cruzi Infection? A Systematic Review of Preclinical and Clinical Evidence. *Parasitology*, **2019**, *146*, 914–927.

[33] Godsel, L.; Leon, J.; Engman, D. Angiotensin Converting Enzyme Inhibitors and Angiotensin II Receptor Antagonists in Experimental Myocarditis. *Curr. Pharm. Des.*, **2003**, *9*, 723–735.

[34] Coelho dos Santos, J.S.; Menezes, C.A.S.; Villani, F.N.A.; Magalhães, L.M.D.; Scharfstein, J.; Gollob, K.J.; Dutra, W.O. Captopril Increases the Intensity of Monocyte Infection by Trypanosoma Cruzi and Induces Human T Helper Type 17 Cells. *Clin. Exp. Immunol.*, **2010**, *162*, 528–536.

[35] Girardi, E.; César-Razquin, A.; Lindinger, S.; Papakostas, K.; Konecka, J.; Hemmerich, J.; Kickinger, S.; Kartnig, F.; Gürtl, B.; Klavins, K.; Sedlyarov, V.; Ingles-Prieto, A.; Fiume, G.; Koren, A.; Lardeau, C.-H.; Kumaran Kandasamy, R.; Kubicek, S.; Ecker, G.F.; Superti-Furga, G. A Widespread Role for SLC Transmembrane Transporters in Resistance to Cytotoxic Drugs. *Nat. Chem. Biol.*, **2020**, *16*, 469–478.

[36] Chaikuad, A.; Koch, P.; Laufer, S.A.; Knapp, S. The Cysteinome of Protein Kinases as a Target in Drug Development. *Angew. Chemie Int. Ed.*, **2018**, *57*, 4372–4385.

[37] Campo, V.A. Comparative Effects of Histone Deacetylases Inhibitors and Resveratrol on Trypanosoma Cruzi Replication, Differentiation, Infectivity and Gene Expression. *Int. J. Parasitol. Drugs Drug Resist.*, **2017**, *7*, 23–33.

[38] Yuan, M.; Li, J.; Lv, J.; Mo, X.; Yang, C.; Chen, X.; Liu, Z.; Liu, J. Polydatin (PD) Inhibits IgE-Mediated Passive Cutaneous Anaphylaxis in Mice by Stabilizing Mast Cells through Modulating Ca2+ Mobilization. *Toxicol. Appl. Pharmacol.*, **2012**, *264*, 462–469.

[39] Valera-Vera, E.A.; Reigada, C.; Sayé, M.; Digirolamo, F.A.; Galceran, F.; Miranda, M.R.; Pereira, C.A. Effect of Capsaicin on the Protozoan Parasite Trypanosoma Cruzi. *FEMS Microbiol. Lett.*, **2020**, *367*.

[40] Markoff, S.; Wilk-Vollmann, S.; Foroutan, B.; Borchardt, C. PGE1-Unterstützte Behandlung Einer Mikrozirkulationsstörung Bei Komplizierter Malaria Tropica. *Anaesthesist*, **2019**, *68*, 683–688.

[41] Parisi, D.; Adasme, M.F.; Sveshnikova, A.; Bolz, S.N.; Moreau, Y.; Schroeder, M. Drug Repositioning or Target Repositioning: A Structural Perspective of Drug-Target-Indication Relationship for Available Repurposed Drugs. *Comput. Struct. Biotechnol. J.*, **2020**, *18*, 1043–1055.

[42] Huryn, D.M.; Resnick, L.O.; Wipf, P. Contributions of Academic Laboratories to the Discovery and Development of Chemical Biology Tools. *J. Med. Chem.*, **2013**, *56*, 7161–7176.

[43] Zhang, D.; Lazim, R. Application of Conventional Molecular Dynamics Simulation in Evaluating the Stability of Apomyoglobin in Urea Solution. *Sci. Rep.*, **2017**, *7*, 44651.

[44] Kumar, N.; Srivastava, R.; Prakash, A.; Lynn, A.M. Structure-Based Virtual Screening, Molecular Dynamics Simulation and MM-PBSA toward Identifying the Inhibitors for Two-

Component Regulatory System Protein NarL of Mycobacterium Tuberculosis. *J. Biomol. Struct. Dyn.*, **2020**, *38*, 3396–3410.

[45] Ornnork, N.; Kiriwan, D.; Lirdprapamongkol, K.; Choowongkomon, K.; Svasti, J.; Eurtivong, C. Molecular Dynamics, MM/PBSA and in Vitro Validation of a Novel Quinazoline-Based EGFR Tyrosine Kinase Inhibitor Identified Using Structure-Based in Silico Screening. *J. Mol. Graph. Model.*, **2020**, *99*, 107639.

[46] Wiggers, H.J.; Rocha, J.R.; Fernandes, W.B.; Sesti-Costa, R.; Carneiro, Z.A.; Cheleski, J.; da Silva, A.B.F.; Juliano, L.; Cezari, M.H.S.; Silva, J.S.; McKerrow, J.H.; Montanari, C.A. Non-Peptidic Cruzain Inhibitors with Trypanocidal Activity Discovered by Virtual Screening and In Vitro Assay. *PLoS Negl. Trop. Dis.*, **2013**, *7*, e2370.

[47] Choe, Y.; Brinen, L.S.; Price, M.S.; Engel, J.C.; Lange, M.; Grisostomi, C.; Weston, S.G.; Pallai, P. V.; Cheng, H.; Hardy, L.W.; Hartsough, D.S.; McMakin, M.; Tilton, R.F.; Baldino, C.M.; Craik, C.S. Development of α-Keto-Based Inhibitors of Cruzain, a Cysteine Protease Implicated in Chagas Disease. *Bioorg. Med. Chem.*, **2005**, *13*, 2141–2156.

[48] Cardoso, M.V.D.O.; Siqueira, L.R.P. De; Silva, E.B. Da; Costa, L.B.; Hernandes, M.Z.; Rabello, M.M.; Ferreira, R.S.; Da Cruz, L.F.; Magalhães Moreira, D.R.; Pereira, V.R.A.; De Castro, M.C.A.B.; Bernhardt, P. V.; Leite, A.C.L. 2-Pyridyl Thiazoles as Novel Anti-Trypanosoma Cruzi Agents: Structural Design, Synthesis and Pharmacological Evaluation. *Eur. J. Med. Chem.*, **2014**, *86*, 48–59.